Journal of
PERIODONTAL RESEARCH

J Periodont Res 2017; 52: 628–635

JOURNAL OF PERIODONTAL RESEARCH
doi:10.1111/jre.12431

In vitro evaluation of the human gingival fibroblast/gingival mesenchymal stem cell dynamics through perforated guided tissue membranes: cell migration, proliferation and membrane stiffness assay

A. Y. Gamal[1], N. N. Al-Berry[1], A. A. Hassan[1], L. A. Rashed[2], V. J. Iacono[3]

[1]Department of Periodontology, Faculty of Dentistry, Ain Shams University, Cairo, Egypt, [2]Faculty of Medicine, Cairo University, Cairo, Egypt and [3]School of Dental Medicine, Stony Brook University, Stony Brook, NY, USA

Gamal AY, Al-Berry NN, Hassan AA, Rashed LA, Iacono VJ. In vitro evaluation of the human gingival fibroblast/gingival mesenchymal stem cell dynamics through perforated guided tissue membranes: cell migration, proliferation and membrane stiffness assay. J Periodont Res 2017; 52: 628–635. © 2017 John Wiley & Sons A/S. Published by John Wiley & Sons Ltd

Background: Migration of gingival fibroblasts/gingival mesenchymal stem cells through macro-perforated barrier membranes may allow them to participate positively in periodontal regeneration. The optimal guided tissue membrane perforation diameter that could favor maximum cell migration into the defect area and at the same time act as an occlusive barrier for gingival epithelium and its associated gingival extracellular matrix component is not yet identified.

Material and Methods: Cultured human gingival fibroblasts/gingival mesenchymal stem cells were placed in the upper chambers of 12-well collagen-coated polytetrafluoroethylene transwells, which were manually perforated with 0.2, 0.4 and 0.7 mm sized pores. The lower chambers of the transwells received blood clot as an attraction medium. The number of cells that have migrated to the lower chambers was calculated. Proliferation of these cells was evaluated using MTT assay. Scanning electron microscopy images were obtained for the lower surfaces of the transwell membranes. Perforated bovine collagen membranes (Tutopatch®) were subjected to mechanical testing to determine the tensile strength and modulus of elasticity.

Results: Group 3 (0.7 mm) showed significantly higher values for cell migration and proliferation. All groups showed a small degree of extracellular matrix migration through membrane perforations. Scanning electron microscopy evaluation revealed variable numbers of cells in fibrin matrices located mainly around the pore edges. There were non-significant differences between groups regarding mechanical properties.

Vincent J. Iacono, DMD, Department of Periodontology, School of Dental Medicine, Stony Brook University, Stony Brook, NY 11794-8703, USA
Tel: 631-632-8895/8955
Fax: 631-632-3113
e-mails: Vincent.Iacono@stonybrook.edu and Vincent.Iacono@sbumed.org

Key words: guided tissue membrane; guided tissue regeneration; periodontal pockets; periodontal regeneration

Accepted for publication October 26, 2016

Conclusions: The present study demonstrated that macro-membrane perforations of 0.2, 0.4 and 0.7 mm are suitable pore diameters that could maintain membrane stiffness and allow for cellular migration. However, these membrane perforation diameters did not allow for total gingival connective tissue isolation.

Gingival tissues have a characteristic and remarkable capacity of wound healing and rapid regeneration. During healing, gingival fibroblasts display multiple functions and can diversely respond to growth factors and produce specific extracellular matrix (ECM) proteins (1). *In vitro*, human gingival fibroblasts were found to express variable levels of mRNA for alkaline phosphatase and bone morphogenetic protein 2/4 (BMP-2/4). When compared to periodontal ligament fibroblasts, gingival fibroblasts showed a higher level of mRNA for BMP-4, while their expression of mRNA for alkaline phosphatase and BMP-2 was similar to that of periodontal ligament fibroblasts (2). To test the regenerative potential of gingival fibroblast, Buurma and coworkers provided evidence that gingival fibroblasts expressed genes responsive to BMP, indicating their capacity of hard tissue formation under appropriate stimuli (3). In addition, Tomar *et al*. demonstrated that human gingiva-derived gingival mesenchymal stem cells (GMSCs) that are usually associated with gingival fibroblasts have several advantages over bone marrow-derived MSCs for cell therapy and regenerative medicine (4). Fawzy El-Sayed *et al*. transplanted autologous GMSCs into periodontal defects created in experimental animals. They reported that these autologous stem/progenitor cells had a significant periodontal regenerative effect, as they showed a remarkable capacity to form bone, cementum and periodontal ligament (1). This multipotent regenerative capacity of the gingival fibroblasts and their associated GMSCs, which is known to be controlled by their surrounding media of gingival ECM, makes it necessary to re-evaluate guided tissue membrane isolation of such cells and develop a tool that allows for gingival fibroblasts/GMSCs to share positively in periodontal regeneration.

The concept of gingival tissue occlusion was tested by Wikesjö *et al*. using an animal model of guided tissue regeneration (GTR). They used macroporous polytetrafluoroethylene (PTFE) membranes with 300 μm pores, 0.8 mm apart and compared them to the occlusive membrane. They concluded that gingival tissue occlusion did not appear as a critical determinant of successful GTR and that macroporous devices may increase the predictability of GTR (5). In a human clinical trial, Gamal and Iacono used perforated collagen membranes for GTR of two- and three-wall intrabony periodontal defects. The membrane was perforated with 0.5–1 mm round holes, 2 mm apart and with a 2 mm occlusive collar at the cervical portion. When compared to occlusive membranes, sites treated by modified perforated membranes showed a significantly greater clinical improvement regarding probing depth reduction and clinical attachment level gain after 9 mo (6–8). Gutta *et al*. examined the effect of barrier's pore size on the outcome of guided bone regeneration. They used titanium meshes with pore sizes of 0.6 and 1.2 mm, and resorbable meshes with a 1 mm pore size. They reported that new bone formation in the group with macroporous (1.2 mm) titanium mesh was significantly higher than in the other groups (9).

The optimal perforation diameter that favors maximum cell migration into the defect area, and at the same time acts as an occlusive barrier for gingival epithelium and gingival ECM component is not yet identified. In this study, three different perforation diameters were evaluated to test gingival fibroblasts and their associated GMSC locomotion and proliferation through resorbable collagen membrane. The main hypothesis is that gingival cell translocation could allow for the gingival fibroblasts/GMSCs to be subjected to the ECM components of the periodontal ligament and bony surfaces of the remaining periodontal structures, altering their behavior in response to periodontal ligament and bone mediators. Perforated membrane stiffness was also evaluated to figure out the membrane perforation diameter that could negatively affect membrane stiffness, which could adversely affect the space keeping effect of the membranes.

Material and methods

Human gingival tissue samples collection

Small biopsies (2 × 2 × 2 mm) of attached gingiva consisting of epithelium and connective tissue were harvested from three healthy adult donors (21, 24, 31 years old) under local anesthesia, during third molar extraction procedure. Samples were then transported to the laboratory in an alpha modification of Eagle's medium (α-MEM) with 10% qualified fetal bovine serum, 1% penicillin, streptomycin and amphotericin (10). Tissues were donated with the patient's informed consent following approval of the procedure by the Research Ethics Committee, Faculty of Dentistry, Ain Shams University.

Gingival fibroblasts/gingival mesenchymal stem cell culturing

The excised tissues were washed in phosphate-buffered saline three times. The epithelial layer was removed by sterile surgical blade and then the specimens were minced into small 1 mm^3 pieces. The minced pieces were collected in sterile, labeled 1.5 mL

Eppendorf tubes into which enzyme digestion was carried out according to Gronthos *et al.* (11), using digesting solution composed of 3 mg/mL collagenase type II (Sigma-Aldrich, St. Louis, MO, USA) for 30–45 min at 37°C. The digestive reaction was stopped by the addition of culture medium. The culture medium consisted of Dulbecco's MEM (DMEM) with L-glutamine supplemented with 10% fetal bovine serum (Gibco, Invitrogen Life Technologies, Waltham, MA, USA), antibiotics (Penicillin G100 units/mL and streptomycin 100 μg/mL) and, finally, an antimycotic agent (fungizone, 0.25 μg/mL).

Single cell suspensions were obtained by passing the digested tissues through a 70 μm cell strainer (Becton Dickinson, Durham, NC, USA). The cells were then centrifuged in an Eppendorf tube at 1440 *g* for 10 min. The cells in the pellet were resuspended in complete culture medium by successive pipetting. All cell fractions were collected and seeded with complete α-MEM (Gibco, Invitrogen Life Technologies) containing 10% fetal bovine serum (Hyclone Laboratories, Inc., Logan, UT, USA), 100 U/mL penicillin, and 100 mg/mL streptomycin in a tissue culture flask ($1–2 \times 10^4$ cells/cm^2) at 37°C in 5% CO_2. After 48 h, cells were washed thoroughly, replaced with fresh medium and fed every 2–3 d.

Gingival fibroblast/gingival mesenchymal stem cell subculturing "passaging"

Passaging was performed when the primary cell culture reached 70% confluence and this was named passage 0. Later passages were named accordingly. Primary cell cultures were treated with a sterile solution of trypsin/EDTA for 5–10 min at 37°C in the incubator and shaken intermittently. Fetal bovine serum (100 μL) was added to inactivate trypsin. The cells were then collected by centrifugation at 6 *g* for 10 min and the cell pellet obtained was resuspended in 1 mL complete medium and divided into two plates (passaging) followed by immersion in complete culture medium to increase cell numbers. Thus, the primary cell culture was propagated and expanded in repeated cell cultures.

Cells were subcultured every other week and the culture medium was replaced every 2–3 d over a 21 d period. Cells were routinely observed under phase-contrast inverted microscope (Leica, Berlin, Germany) and no epithelial cells were found by microscopy in the primary and passaged cultures. Daily follow-up of gingival fibroblasts with their associated stem cells was done to ensure cell viability. Cell proliferation was monitored in primary cultures and subcultures. The proliferation capacity was judged by close follow-up of the confluence rate, i.e. culture plates reaching 70% confluence according to culture days. The final population doubling value for the gingival fibroblast and its associated GMSC-like cells was represented as the sum of population doubling values obtained at each passage for three successive passages. The experiments were done in triplicate.

Gingival mesenchymal stem cell colony formation efficiency, morphology, adherence and stem cell surface markers testing

Gingival fibroblasts with their associated GMSC-like cells at the fifth passage were observed under inverted light microscope. Aggregates with more than 50 cells were scored as colonies. To examine the cell appearance and measurements, morphometrical analysis by means of light microscopy was conducted. The first adherent cells appeared at day 6. The cells showed spindle-shaped, fibroblast-like morphology under the light microscope. GMSCs displayed plastic adherence to tissue culture flasks. For identification of the MSC phenotype, approximately 5×10^5 cells were incubated with phycoerythrin- or fluorescein isothiocyanate-conjugated monoclonal antibodies for human CD34, CD29 (eBioscience, San Diego, CA, USA), fluorescein isothiocyanate-conjugated CD146 (R&D Systems, Inc., Minneapolis, MN, USA) or isotype-matched control IgGs. Cells were subjected to flow cytometric analysis using a Beckman Coulter Epics XL (Beckman Coulter, Fullerton, CA, USA).

Gingival fibroblast/gingival mesenchymal stem cell migration assay

Cell migration assay was performed in a collagen-coated PTFE 12-transwell chemotaxis chamber(s) (Corning Life Sciences, Corning, NY, USA), 12 mm in diameter. The membranes were manually perforated, with 2 mm inter-perforation distance. They were divided into three groups according to the perforation diameter: group 1, 0.2 mm perforations; group 2, 0.4 mm perforations; and group 3, 0.7 mm perforations. An acrylic stent with 2 mm inter-perforation distances of the same chemotactic chamber diameter was fabricated and used for manual perforations using customized 0.2, 0.4 and 0.7 mm pins. Cells were harvested using phosphate-buffered saline containing 0.2 mg/mL EDTA and resuspended in DMEM containing 1% fetal calf serum. The upper chamber of the transwell was loaded with 120,000 cells in Matrigel. The lower chamber received the attraction medium (blood clot + 1% fetal calf serum/DMEM). The cultures were maintained at 37°C under 5% CO_2 for 48 h. Cells on the upper surface of the membrane were removed by a cotton swab and cells that migrated to the lower side were fixed with methanol and stained with 0.1% crystal violet. In 1 mL tube 0.2% of Trypan Blue stain (Sigma-Aldrich, Haverhill, UK) was mixed with the cell suspension and incubated for 5 min at room temperature, then placed on a Neubauer hemocytometer. The cells were counted under an inverted microscope and the cell numbers were multiplied with sample values to calculate the total cell number.

MTT cell proliferation assay

MTT assay is based on the reduction of tetrazolium salts, and it is now widely accepted as a reliable method for examining cell proliferation (12). The resultant intracellular purple

formazan can be solubilized and quantitated by spectroscopic means. The MTT reagent yields low background absorbance values in the absence of cells and is stable when stored at 4°C. Cell proliferation was assessed as the percentage of cell proliferation compared to control, which was considered as 100%.

The cell proliferation assay was measured after 48 h. Cells in the lower chambers of the transwells were incubated with 10 μL MTT reagent (cat. no. 4890-25-01) (Trivigen Inc., Gaithersburg, MD, USA), for 60 min at 37°C in 96-well plates, until the purple precipitate was clearly visible. Then, 100 μL detergent reagent (cat. no. 4890-25-02) was added to each well to solubilize the formazan dye before measuring the absorbance of each sample. The extent of reduction of MTT to formazan within cells was quantified by using a spectrophotometer at a wavelength of 572 nm. Absorbance is directly proportional to the number of living cells in the specimen.

Scanning electron microscopy of perforated membranes

The lower surfaces of the membranes for the three groups (six samples per group) were prepared for scanning electron microscopy (SEM) imaging. Cells on the upper surface of the membrane were removed with a cotton swab, and then samples were fixed by glutaraldehyde 2.5% and dehydrated by serial dilution of ethanol using automatic tissue processor (Leica EM TP; Leica Microsystems, Berlin, Germany). Samples were then dried using CO_2 critical point drier (Autosamdri®-815; Tousimis, Maryland, USA) and coated by gold spatter coater (SPI-Module; Structure Probe, Inc., West Chester, PA, USA). Finally, samples were examined by SEM (JEOL-JSM-5500 LV; JEOL Inc., Peabody, MA, USA) using the high vacuum mode.

Mechanical testing of the membranes

The tension test was used to determine mechanical properties of perforated collagen membranes compared to non-perforated membranes (control group), under hydrated conditions. The membranes (Tutopatch®; Tutogen Medical GmbH, Germany) were cut into rectangular strips (5 × 30 mm). The thickness of the specimen was measured at three different positions and the average thickness was taken to calculate the cross-sectional area of the specimen. Each sample ($n = 6$ specimens) was hydrated and then loaded into the testing fixture of a Universal Testing Machine (Lloyd instruments LR5, Fareham, UK). Tension was applied at a cross-head speed of 10 mm/min (13) until failure. The stress vs. strain curve was generated. The tensile strength of the specimen was calculated by dividing the maximum stress over the cross-sectional area of the specimen. The elastic modulus was determined by obtaining the slope of the most linear portion of the curve for each specimen: Modulus of elasticity = stress/strain (14).

Statistical analysis

Numerical data were explored for normality by checking the data distribution, calculating the mean and median values and using Kolmogorov–Smirnov and Shapiro–Wilk tests. Data were presented by mean and SD values. Data showing normal distribution were analyzed using one-way ANOVA followed by the Tukey *post-hoc* test, while non-normally distributed data were analyzed using the Kruskal–Wallis test followed by the Mann–Whitney test with a Bonferroni correction. The significance level was set at $p \leq 0.05$. Statistical analysis was performed with SPSS Statistics Version 20 for Windows (IBM Corp., Armonk, NY, USA).

Results

Table 1 demonstrates mean values of total mixed cell migration and proliferation (gingival/GMSC) for each of the studied groups after 48 h. Group 3 (0.7 mm) showed the highest cell migration value followed by group 2 (0.4 mm) and group 1 (0.2 mm). Data for the cell count did not show normal distribution, so Kruskal–Wallis test was used to compare between groups followed by *post-hoc* test. Kruskal–Wallis test showed a significant difference between studied groups. The *post-hoc* test showed a significant difference between group 1 and group 3. Group 3 showed the highest value of cell proliferation followed by group 2 followed by group 1. The data were normally distributed, and the one-way ANOVA test showed a significant difference between studied groups. The *post-hoc* test showed a significant difference between group 1 and group 3.

Flow cytometric analysis was carried out for characterization of stem cells within the cell culture. Figure 1 represents fluorescence intensity for CD146, CD29 and CD34. The cells were positive for mesenchymal surface markers CD146 and CD29, and showed negative expression of hematopoietic cell surface marker CD34 (Fig. 1).

Figure 2 shows the mean tensile strength and modulus of elasticity for each group. Group 1 showed an average tensile strength of 5 ± 0.65 MPa and modulus of 2.32 ± 0.24 MPa while group 2 showed an average tensile strength of 4.36 ± 2.41 MPa and modulus of 2.49 ± 0.83 MPa. Group 3 and control group showed an average tensile strength of 4.26 ± 0.78 and 3.88 ± 1.74 MPa, and modulus

Table 1. Values of cell count and cell proliferation

Assay	Group	Mean	SD	SE
Cell count	G1 (0.2 mm)	14.93s	4367.25	0.022k
	G2 (0.4 mm)	24.88ns	11,686.23	
	G3 (0.7 mm)	42.31s	17,053.31	
Cell proliferation (%)	G1 (0.2 mm)	69.69s	7.15	0.009a
	G2 (0.4 mm)	75.46ns	8.94	
	G3 (0.7 mm)	87.20s	5.36	

K, Kruskal–Wallis test; a, one-way ANOVA; s, significant difference; ns, non-significant difference.

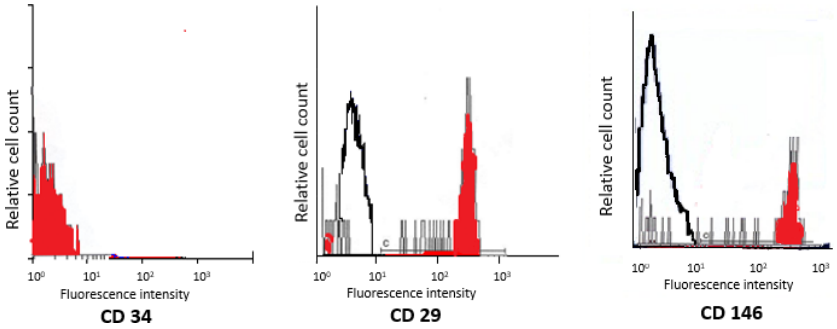

Fig. 1. Flow cytometry analysis of stem cell surface markers.

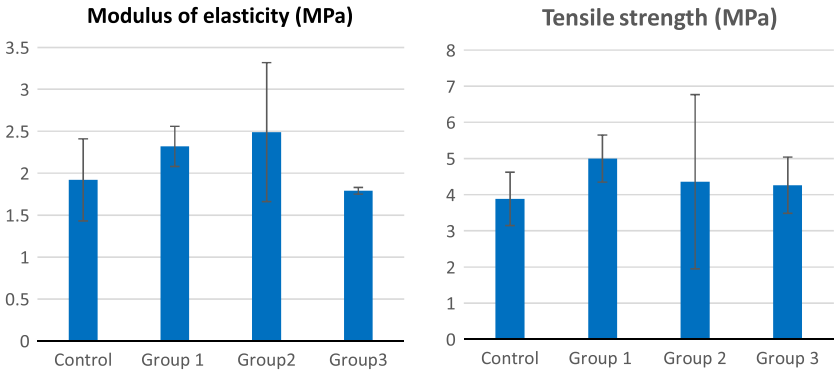

Fig. 2. Mechanical properties of perforated collagen membranes (Tutopatch®).

of 1.79 ± 0.04 and 1.92 ± 0.49 MPa respectively. One-way ANOVA showed no significant difference between studied groups for both tensile strength and modulus of elasticity. Stress/strain curves for the membranes in different groups were presented in Fig. 3.

SEM evaluation revealed uniform perforation diameters in each group in spite of their irregular inconsistent outlines. Aggregates of blood elements and variable numbers of fibroblasts in fibrin matrices on all samples for all groups were observed (Fig. 4). These aggregates were found mainly on the peripheries of the perforations rather than on the membrane surface (Fig. 5A). All groups showed limited numbers of flat polyhedral cells with long cytoplasmic extensions attached to the membrane surfaces (Fig. 4). Some membranes showed a limited number of perforations with gingival fibroblasts and their associated Matrigel matrix protruding out into the lower compartment (Fig. 5B).

Discussion

Critical sized periodontal and alveolar bone defects usually suffer limited regenerative capacity owing to their limited cellularity and the lack of adequate space provision. Periodontal defects and deficient alveolar ridges that are usually overlaid by highly vascular and cellular gingival connective tissue or periosteum respectively are commonly treated by occlusive membranes. This could isolate these cell-deficient defects from a huge source of regenerative elements that could positively share in their reconstruction or regeneration. To allow only positive cellular and biological elements to migrate into the defect area leaving gingival tissue ECM components above the membrane, Gamal and Iacono suggested the use of perforated barrier membranes for the treatment of intrabony defects. They claimed that, membrane perforations may allow for the participation of cells derived from the gingiva (particularly GMSCs and endothelial cells) and periosteum in the regenerative process (6). The present study was conducted to prove feasibility of selective gingival fibroblasts and GMSC migration through selected perforation diameters of collagen membranes. This will allow for selection of the optimal pore diameter that permits maximum cellular migration and minimum gingival connective tissue defect invasion. In this proof of principle study, the cell migration assay was performed in a collagen-coated PTFE 12-transwell chemotaxis chamber to get provisional information about the feasibility of cellular migration through membrane perforations. More studies on customized chemotactic chambers using commercially available collagen membranes are recommended. On the other hand, mechanical properties of perforated membranes were performed on the commercially available collagen membranes.

To achieve optimal outcomes of perforated GTR and bone regeneration membranes, it was important to test the optimal pore diameter that allows for maximum cell migration through membrane perforations without allowing for the passage of the rapidly growing gingival connective tissue, thus preventing pressure atrophy over the newly formed tissue in the defect area. In previous studies performed by the same group, non-evidence–based arbitrary perforations ranged from 0.5 to 1 mm were used (6–8). The present study suggested smaller pore diameters of 0.2, 0.4 and 0.7 mm in an attempt to figure out the optimal perforation diameter. Using an *in vitro* cell migration model, cultured gingival fibroblasts and GMSCs in Matrigel ECM proteins were allowed to migrate through perforated collagen-coated PTFE membranes in transwell chemotaxis chambers in response to blood clot as an attraction medium. Matrigel migration is used to mimic the unwanted ECM migration through membrane perforations (15). Blood clot fibrin strands serve as the matrix for cellular migration. The blood clot also has a powerful chemotactic potential through its content of

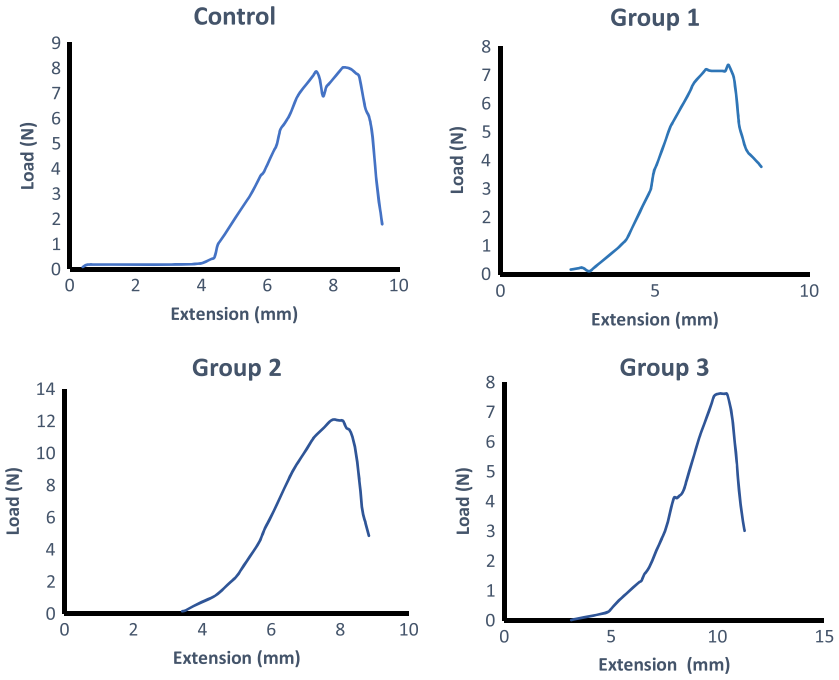

Fig. 3. Stress/strain curves for representative samples of membranes in different groups.

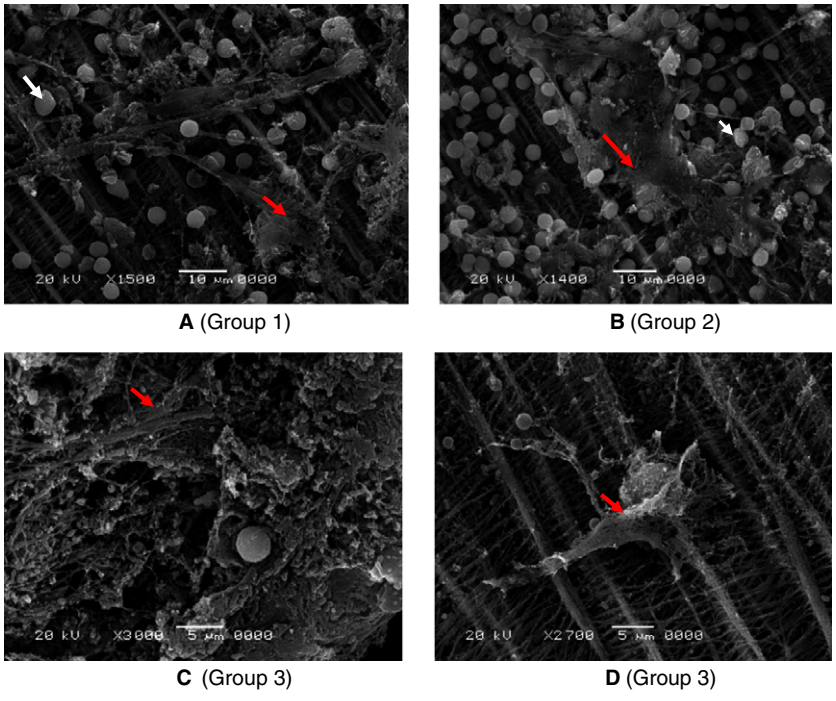

Fig. 4. Scanning electron microscopy image showing fibroblastic migration through different perforation diameters and its attachment to the lower surface of the membrane.

growth factors (16,17). Along with growth factors, the clot matrix molecules function to stimulate the proliferation of wound fibroblasts and provide signals for gene expression, which induce expression of appropriate integrin receptors on the fibroblasts, which are essential for cellular migration (18).

The present study showed that, all pore diameters allowed migration of cells into the lower compartments of transwell chambers. There was a significant difference in the cell migration and proliferation between the three groups. Cell passage through the selected perforation diameters is supported by the study of Irwin *et al.* who studied the morphologic characteristics of fibroblasts obtained from papillary and reticular layers of human gingival tissue. They reported a much smaller size of gingival fibroblasts than the selected pore diameters. Papillary fibroblasts reported to have an average size of 81 ± 21 μm, while the reticular fibroblasts were 210 ± 56 μm (19). The present study showed also in SEM analysis extrusion of Matrigel ECM through membrane perforations in few perforations for all groups. This finding suggests that more predictable outcomes could be achieved than of the same group's previous clinical findings by more adjustment of membrane perforations to be totally occlusive for gingival connective tissue elements. Studying smaller perforation diameters that could totally obstruct connective tissue invasion is currently under investigation by the same group.

The cell proliferation assay was done for the migrating cells to ensure their viability and activity following their translocation into another medium, which is the blood clot in the lower compartments. Group 1 showed a mean proliferation rate of 69%, group 2 showed 75%, while group 3 showed 87%. These gradually increasing percentages were proportional with the reported finding of a significant increase in migrating cell numbers that was associated with increasing perforation diameter. These data also confirm the possibility of cell migration through membrane perforations to share positively in the process of regeneration to compensate for the limited cellularity of the periodontal defect. It also throws light on the importance of chemotactic media availability at the lower compartment of the defect to allow for more cellular migration to the cell-deficient compartment below the membrane. This finding also supported the outcomes of studies by Gamal *et al.* that reported higher gingival crevicular

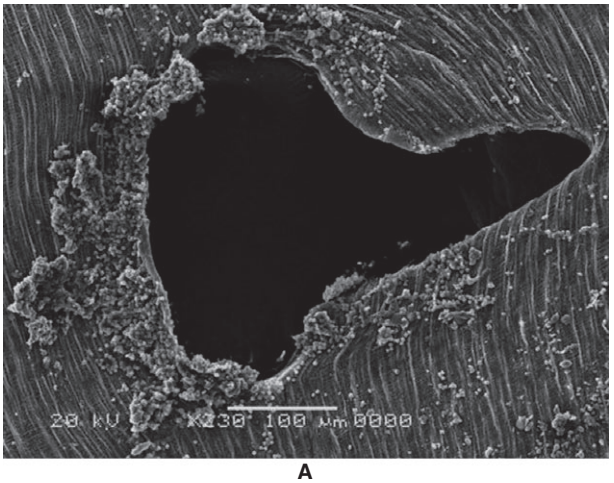

A

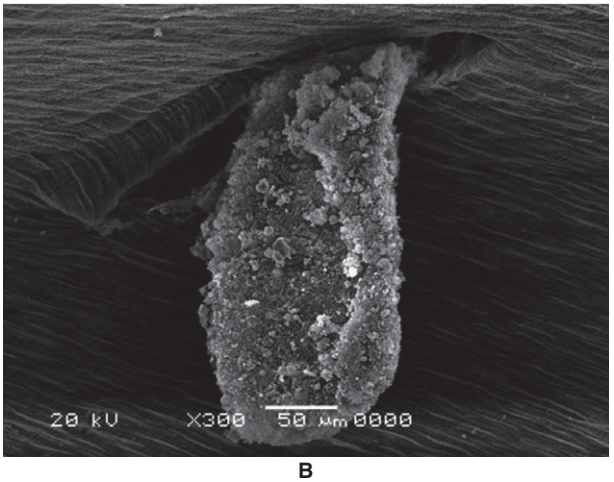

B

Fig. 5. (A) Scanning electron microscopy image of the lower surface of the membranes, showing irregular outline of the perforation and location of cellular aggregates at the peripheries (magnification ×230). (B) Scanning electron microscopy showing an aggregate of blood clot and cellular elements protruding from the center of the perforation denoting the limited connective tissue occlusive capacity of the selected pore diameters (magnification ×300).

fluid levels of BMP-2, vascular endothelial growth factor and platelet-derived growth factor-BB following the use of perforated membranes as compared to an occlusive one (7,8). These higher mediator values could be related to migrating cells through membrane perforations reported in the present study.

SEM examination of the lower surfaces of the membranes showed variable numbers of fibroblasts and blood elements, mainly around the edges of membrane pores, which indicate the route of cell passage through perforation. This could also explain the role of membrane perforations in improving membrane stability. The adherence of connective tissue cells to the inside of a membrane was found to promote periodontal regeneration (20) and an attachment can help to stabilize the blood clot and integrate the membrane into the tissue (21). On the other hand, the whole surface of the membrane did not show a considerable number of attached cells. This could be attributed to the design of the transwells used, as the lower chambers provided a space containing nourishing culture medium and blood clot, which may attract the cells to move to this available space rather than attaching to the membrane surface. This finding throws light on the importance of chemotactic factor availability below the membrane, which is supposed to prevent cellular adherence to the membrane and allow it to pass into the defect area to be differentiated in response to periodontal tissue mediators. GMSC adherence to collagen membrane may allow for unwanted differentiation into soft tissue forming cells.

An ideal resorbable membrane should facilitate the attachment, proliferation and migration of cells on its outer surface to seal the underlying defect off from the oral flora, even in the case of membrane exposure. In the present study, data from positive cell migration and maintenance of cell viability could convert the role of a guided tissue membrane from being a totally mechanical device into a membrane filter that is mechanically obstructive for unwanted gingival connective tissue elements and biologically permeable for regenerative cellular and biological elements.

An SEM finding of uniform perforation diameters in each group in spite of their irregular inconsistent outlines suggests the need for a modality that is more reliable for perforating membranes during manufacturing. Mechanical testing was also done to determine the effect of membrane perforations on membrane stiffness, which could affect the space making properties of the membrane. As stated by Scantlebury (22), space provision and maintenance are essential design criteria for membranes used in GTR. He reported that the contour and volume of new bone formed in the defects is determined by the space created and protected by the barrier membrane. Membrane stiffness prevents its collapse into the defect. Schenk *et al.* reported that guided bone regeneration membranes, which demonstrated significant collapse, resulted in smaller available space for new bone formation in mandibular bone defects in dogs (23). Inter-pore distance was determined as suggested by Gamal and Iacono (6) of 2 mm as a provisional measure that lacks pre-clinical supportive evidence to preserve membrane stiffness.

In the present study, all groups showed non-significant differences when compared with non-perforated ones regarding the tensile strength and modulus of elasticity ($p > 0.05$). These data indicated that the design of membrane perforations used in this study did not affect membrane stiffness and accordingly the space making properties of the membrane.

Within the limits of the present study, we can conclude that macromembrane perforations of 0.2, 0.4 and 0.7 mm are suitable pore diameters that could maintain membrane stiffness and allow for cellular migration. However, these membrane perforation diameters do not allow for total gingival connective tissue isolation. This could affect negatively the optimal outcomes of perforated membrane use. More investigations are required to test smaller membrane diameters to reach the ideal perforation diameter that could be totally occlusive for gingival connective tissue elements and permeable for gingival fibroblasts with their associated mediators and GMSC populations. A membrane perforation diameter that allows for selective GMSC migration needs also to be investigated.

Acknowledgement

The authors would like to thank staff of the Department of Biomaterials, Faculty of Dentistry, Ain Shams University for their help in testing membrane rigidity.

Conflict of interest and source of funding

The authors report no conflicts of interest and absence of external funding. The study was funded by the author's own institution.

References

1. Fawzy El-Sayed K, Paris S, Becker S *et al*. Periodontal regeneration employing gingival margin-derived stem/progenitor cells: an animal study. *J Clin Periodontol* 2012;**39**:1–10.
2. Ivanovski S, Li H, Haase H, Bartold P. Expression of bone associated macromolecules by gingival and periodontal ligament fibroblasts. *J Periodontal Res* 2001;**36**:131–141.
3. Buurma B, Gu K, Rutherfold R. Transplantation of human pulpal and gingival fibroblasts attached to synthetic scaffolds. *Eur J Oral Sci* 1999;**107**:282–289.
4. Tomar GB, Srivastava RK, Gupta N *et al*. Human gingiva-derived mesenchymal stem cells are superior to bone marrow-derived mesenchymal stem cells for cell therapy in regenerative medicine. *Biochem Biophys Res Commun* 2010;**393**:377–383.
5. Wikesjö UME, Lim WH, Thomson RC, Hardwick WR. Periodontal repair in dogs: gingival tissue occlusion, a critical determinant for GTR? *J Clin Periodontol* 2003;**30**:655–664.
6. Gamal AY, Iacono VJ. Enhancing guided tissue regeneration of periodontal defects by using a novel perforated barrier membrane. *J Periodontol* 2013;**84**: 905–913.
7. Gamal AY, Aziz M, Iacono VJ. Gingival crevicular fluid bone morphogenetic protein-2 release profile following the use of perforated membrane barriers in localized intrabony defects: a randomized clinical trial. *J Int Acad Periodontol* 2014;**16**:1–9.
8. Gamal AY, Abdel-Ghaffar KA, Iacono VJ. Gingival crevicular fluid vascular endothelial cell growth factor and platelet-derived growth factor-BB release profile following the use of perforated barrier membranes during treatment of intrabony defects: a randomized clinical trial. *J Periodontal Res* 2016;**51**:407–416.
9. Gutta R, Baker RA, Bartolucci AA, Louis PJ. Barrier membranes used for ridge augmentation: is there an optimal pore size? *J Oral Maxillofac Surg* 2009;**67**:1218–1225.
10. Mitrano TI, Grob MS, Carrio F *et al*. Culture and characterization of mesenchymal stem cells from human gingival tissue. *J Periodontol* 2010;**81**:917–925.
11. Gronthos S, Agnieszka A, Bartold PM, Shi S. A method to isolate and culture expand human dental pulp stem cells. In: *Mesenchymal Stem Cell Assays and Applications, Methods in Molecular Biology*, Vol. 698, Philadelphia: Springer Science + Business Media, LLC, 2011:107–121.
12. van Meerloo J, Kaspers GJ, Cloos J. Cell sensitivity assays: the MTT assay. In: Cree IA, ed. *Cancer Cell Culture Methods Protocols, Second Edition, Methods in Molecular Biology*, Vol. 791, Philadelphia: Springer Science + Business Media, LLC, 2011:237–245.
13. Kuo SM, Chang SJ, Cheng-Chie Niu G, Lan CW, Cheng WT, Yang CZ. Guided tissue regeneration with use of β-TCP/chitosan composite membrane. *J Appl Polym Sci* 2009;**112**:3127–3134.
14. McCabe JF, Walls AW. Properties used to characterise materials. In: McCabe JF, Walls AW, eds. *Applied Dental Materials*. Oxford: Blackwell Publishing Ltd., 2008:6–18.
15. Hughes C, Postovit L, Lajoie G. Matrigel: a complex protein mixture required for optimal growth of cell culture. *Proteomics* 2010;**10**:1886–1890.
16. Diegelmann RF, Evans MC. Wound healing: an overview of acute, fibrotic and delayed healing. *Front Biosci* 2004;**9**:283–289.
17. Enoch S, Leaper DJ. Basic Science of wound healing. *Surgery* 2007;**26**:31–37.
18. Clark RA. Fibrin and wound healing. *Ann N Y Acad Sci* 2001;**936**:355–367.
19. Irwin CR, Picardo M, Ellis I *et al*. Inter- and intra-site heterogeneity in the expression of fetal-like phenotypic characteristics by gingival fibroblasts: potential significance for wound healing. *J Cell Sci* 1994;**107**:1333–1346.
20. Machtei EE, Cho MI, Dunford R, Norderyd J, Zambon JJ, Genco RJ. Clinical, microbiological and histological factors which influence the success of regenerative periodontal therapy. *J Periodontol* 1994;**65**:154–161.
21. Wikesjö UME, Sigurdsson TJ, Lee MB, Tatakis DN, Selvig KA. Dynamics of wound healing in regenerative periodontal therapy. *J Calif Dent Assoc* 1995;**23**:30–35.
22. Scantlebury TV. 1982–1992: a decade of technology development for guided tissue regeneration. *J Periodontol* 1993;**64**:1129–1137.
23. Schenk RK, Buser D, Hardwick WR, Dahlin C. Healing pattern of bone regeneration in membrane protected defects: a histologic study in dogs. *Int J Oral Maxillofac Implants* 1994;**9**:13–29.